International Transactions on Electrical Engineering and Computer Science
N. T. Thanh et.al., Vol: 4, No: 1, pp: 25-31, March 2025

Design of a Predictive Controller for the Current Loop of the Tubular Linear Motor Using a Discrete Model

Nguyen Trung Thanh[1], Nguyen Minh Cuong[2], Le Thi Thuy Ngan[1], Duong Quoc Tuan[1]

Abstract: This article proposes a control strategy based on a Constrained Control Set Model Predictive Controller (CCS-MPC) to optimize the control signal while adhering to output limitations. A mathematical model of the tubular linear motor is introduced as the foundation for the controller design. The controller focuses on the internal control loop, which is directly affected by the converter's limitations. The performance of the proposed controller is validated through simulations in MATLAB/Simulink, demonstrating its effectiveness with a current response time of less than 200 μs.

Keywords: CCS-MPC, Tubular linear motor, Linear Motor

1. Introduction

In recent years, various types of linear motors have been extensively studied. The primary advantage of these motors is their ability to generate direct translational force without requiring mechanical transmission structures. This characteristic eliminates intermediate mechanisms, reduces the size of the drive system, enhances precision, minimizes energy loss, and lowers costs and maintenance expenses [1-3].

Article History
Received: 15-11-2024; Revised: 08-02-2025;
Accepted: 25-02-2025

Nguyen Trung Thanh
nguyentrungthanh@tnut.edu.vn

[1]Faculty of Mechanical, Electrical, Electronics Technology, Thai Nguyen University of Technology, Thai Nguyen City – 251750, Vietnam.
[2]Faculty of Electrical Engineering, Thai Nguyen University of Technology, Thai Nguyen City – 251750, Vietnam.

Similar to rotary motors, traditional control strategies such as Field Oriented Control (FOC), Direct Torque Control (DTC), and V/f control have been applied to linear motors [4 - 9]. However, nonlinear effects such as end effects and slot effects pose significant challenges for linear controllers like the PI controller [10 - 12]. As a result, advanced controllers have been developed and implemented. In particular, sliding mode controllers based on Lyapunov stability principles have been successfully applied, demonstrating fast response and stability under load variations while mitigating undesirable effects [13 - 16]. However, these controllers require precise model parameters to generate appropriate control signals. To address model uncertainties, observer-based controllers have been employed [14 - 17], and machine learning models have also been used to estimate model parameters [18 - 19]. Most existing control solutions assume that the power converter behaves as a proportional gain system with a constant amplification factor. However, power converters are limited by switching vectors and the DC-Link bus voltage, which constrain control signals. This directly impacts the performance of the inner-loop current controller. Therefore, an optimal selection of control signals is essential.

https://doi.org/10.62760/iteecs.4.1.2025.123

In this paper, a CCS-MPC control structure is developed to optimize control signals while considering output constraints. The next section presents a mathematical model of the tubular linear motor as the foundation for designing the proposed controller. Finally, a simulation model is built in MATLAB/Simulink to validate the controller's effectiveness.

The remaining paper organized into various sections. Section 2 about the suggested discrete controller, Section 3 simulation results and in Section 4 the conclusions are presented.

2. Proposed Discrete Controller

2.1 Mathematical Model

A tubular linear motor consists of a slider acting as the rotor and windings acting as the stator as in Fig. 1 (a). The stator comprises windings wound around the main drive shaft, while the rotor consists of axially magnetized permanent magnet segments arranged in sequence. The motor moves flexibly along its axis. The internal structure and key parameters of the linear motor are depicted in Fig. 1 (b).Each pole pitch has a length of τ and consists of three-phase windings (a, b, c). The width of each winding is one-third of the pole pitch. In linear motors, the magnetized section of the rotor is designed to be longer than the stator to ensure uniform flux distribution across the stator windings. The effective interaction length between the stator and rotor is denoted as l_{eff}, and the rotor diameter D must be smaller than the stator diameter.

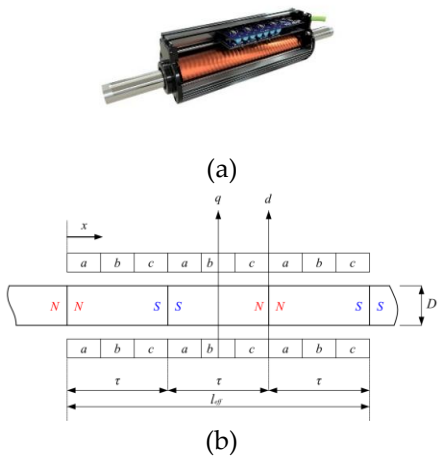

Fig. 1: Tubular linear motor

The mathematical model of the tubular linear motor is based on electromagnetic principles and is expressed in the dq reference frame as follows (1) [20].

$$\begin{cases} \dfrac{di_d}{dt} = \dfrac{u_d}{L_s} - \dfrac{R_s}{L_s} i_d + \omega_r i_q \\ \dfrac{di_q}{dt} = \dfrac{u_q}{L_s} - \dfrac{R_s}{L_s} i_q - \omega_r i_d - \dfrac{\omega_r}{L_s} \psi_f \end{cases} \quad (1)$$

Where: i_d, i_q and u_d, u_q are current and voltage on dq-coordinate, respectively; ψ_f is the flux linkage generated by the rotor's permanent magnets; ω_r is the rotor's angular velocity, given below,

$$\omega_r = \frac{\pi}{\tau} v$$

where v is the linear velocity of the rotor.

The thrust force is given by (2)

$$F_T = \frac{3}{2} \frac{\pi p}{\tau} k_F \left[\psi_d i_q - \psi_q i_d \right] \quad (2)$$

Where p is the number of pole pairs, and k_F is the thrust coefficient, ψ_d ψ_q are the d-axis and q-axis magnetic flux components of the permanent magnets. For controller design, the system equations (1) are rewritten in matrix form as below,

$$\frac{d\mathbf{i}_{dq}}{dt} = \mathbf{T}\mathbf{i}_{dq} + \mathbf{L}\mathbf{u}_{dq} + \mathbf{W}\mathbf{i}_{qd}\omega_r + \mathbf{P}\psi_f\omega_r \quad (3)$$

where

$$\mathbf{i}_{dq} = \begin{bmatrix} i_d & i_q \end{bmatrix}^T ; \ \mathbf{i}_{qd} = \begin{bmatrix} i_q & i_d \end{bmatrix}^T ; \ \mathbf{T} = \begin{bmatrix} \frac{R_s}{L_s} \end{bmatrix} ;$$

$$\mathbf{L} = \begin{bmatrix} \frac{1}{L_s} \end{bmatrix} ; \ \mathbf{W} = \begin{bmatrix} 0 & 1 \\ -1 & 0 \end{bmatrix} ; \ \mathbf{P} = \begin{bmatrix} 0 \\ -1 / L_s \end{bmatrix}$$

Equation (3) describes the electrical part of the tubular linear motor in the dq coordinate system, rotating synchronously with the motor's rotor. For the convenience of the controller design process, we choose the d-axis to coincide with the magnetic flux axis of the rotor's magnet. Therefore, the motor model (2) and (3) can be rewritten as follows (4) and (5),

$$\frac{d\mathbf{i}_{dq}}{dt} = \mathbf{T}\mathbf{i}_{dq} + \mathbf{L}\mathbf{u}_{dq} + \mathbf{W}\mathbf{i}_{qd}\omega_r + \mathbf{P}\psi_f\omega_r \quad (4)$$

and

$$F_T = \frac{3}{2}\frac{\pi p}{\tau}k_F\psi_f i_q \quad (5)$$

In equation (5), the thrust is determined solely by the current i_q. Therefore, a control structure based on the principle of rotor magnetic flux will be introduced in the next section.

2.2 Controller Design

By aligning the dq reference frame with the rotor flux, a cascade control structure is developed: an outer speed control loop and an inner current control loop. The proposed control strategy is illustrated in Fig. 2. The speed control loop is designed using conventional algorithms, while the current control loop accounts for the discrete nature of the current and converter limitations. As with traditional control strategies, PI controllers are used for the speed and position loops. However, the current loop requires improvement for enhanced performance, using an advanced algorithm. An FCS-MPC controller is implemented to address these challenges. The controller design steps are presented. Using a Taylor series expansion, the discrete model is obtained as (6)

$$\begin{aligned}\mathbf{i}_{dq}(k+1) &= \mathbf{i}_{dq}(k) + \mathbf{T}_s\mathbf{i}_{dq}(k) + \mathbf{L}_s\mathbf{u}_{dq}(k) \\ &\quad + \mathbf{W}_s\mathbf{i}_{qd}(k)\,\omega_r(k) + \mathbf{P}_s\psi_f\omega_r(k)\end{aligned} \quad (6)$$

Where:

$$\mathbf{T}_s = T_s\begin{bmatrix}\frac{R_s}{L_s}\end{bmatrix} \;;\; \mathbf{L}_s = T_s\begin{bmatrix}\frac{1}{L_s}\end{bmatrix} \;;\; \mathbf{W}_s = T_s\begin{bmatrix}0 & 1\\ -1 & 0\end{bmatrix} \;;$$
$$\mathbf{P}_s = T_s\begin{bmatrix}0\\ -1/L_s\end{bmatrix}$$

T_s is the sampling time of the current, typically equal to the carrier frequency of the converter. From the discrete model (6), we can rewrite it as follows (7)

$$\begin{aligned}\mathbf{i}_{dq}(k+1) &= \mathbf{i}_{dq}(k) + \mathbf{T}_s\mathbf{i}_{dq}(k) + \mathbf{W}_s\mathbf{i}_{qd}(k)\,\omega_r(k) \\ &\quad + \mathbf{L}_s\mathbf{u}_{dq}(k) + \mathbf{P}_s\psi_f\omega_r(k) \\ &= \mathbf{\Phi}\mathbf{i}_{dq}(k) + \mathbf{L}_s\mathbf{u}_{dq}(k) + \mathbf{P}_s\psi_f\omega_r(k)\end{aligned} \quad (7)$$

Where

$$\mathbf{\Phi} = T_s\left[\mathbf{I} + \mathbf{T}_s + \mathbf{W}_s\omega_r(k)\right]$$

Based on the discrete model (7), a current estimation model is created as follows (8)

$$\begin{aligned}&\mathbf{i}_{dq}^{est}(k+i+1\,|\,k) = \\ &\mathbf{\Phi}\mathbf{i}_{dq}^{est}(k+i\,|\,k) + \mathbf{L}_s\bar{\mathbf{u}}_{dq}(k) + \mathbf{P}_s\psi_f\omega_r(k)\end{aligned} \quad (8)$$

Where $\mathbf{i}_{dq}^{est}(k) = \mathbf{i}_{dq}(k)$ s the current at the k[th] sampling time; $\bar{\mathbf{u}}_{dq}(k+i)$ is the next control signal at the i[th], with a prediction range N.

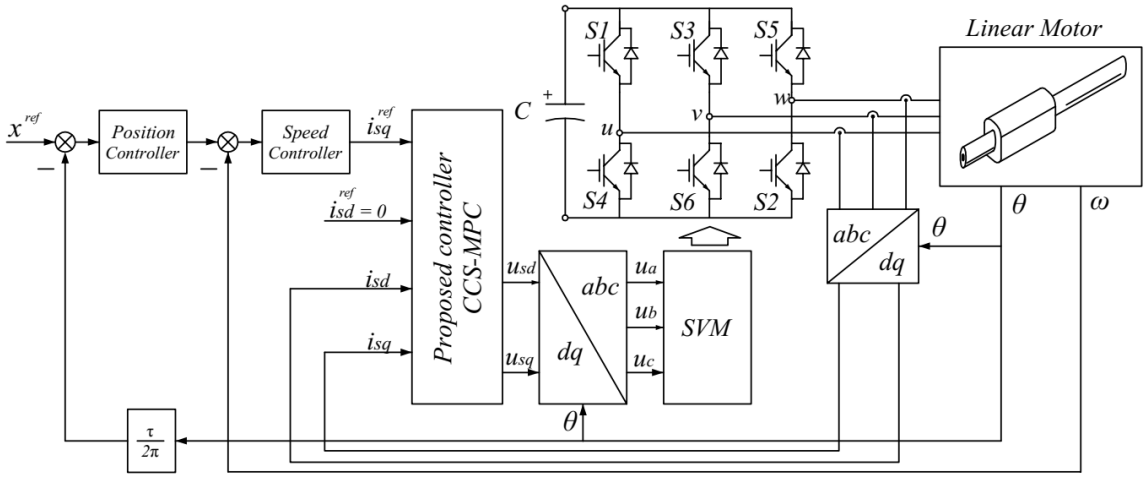

Fig. 2: The proposed control strategy.

The purpose of the controller is to find an optimal control value. To achieve this, we select a quadratic cost function, expressed as follows (9)

$$J = \sum_{i=1}^{N} \left[\mathbf{i}_{dq}^{ref} - \mathbf{i}_{dq}^{est} \ k+i \ \ \mathbf{Q} \ \mathbf{i}_{dq}^{ref} - \mathbf{i}_{dq}^{est} \ k+i \ \right] \quad (9)$$

where $\mathbf{Q} = \begin{bmatrix} \lambda & 0 \\ 0 & 1 \end{bmatrix}$ is a positive definite diagonal weight matrix, the coefficient λ_d is the weight of the error in the objective function J. And i_{dq}^{ref} are the output of the speed controller. The control voltage udq is constrained by the inverter modulation strategy using Space Vector Modulation (SVM), with six fundamental voltage vectors forming a hexagonal boundary as shown in Fig. 3. With this method, the modulation values will be normalized to form a vector: $\mathbf{u}_s = \begin{bmatrix} u_a & u_b & u_c \end{bmatrix}^T$ where $|u_a|, |u_b|, |u_c| < 1$.

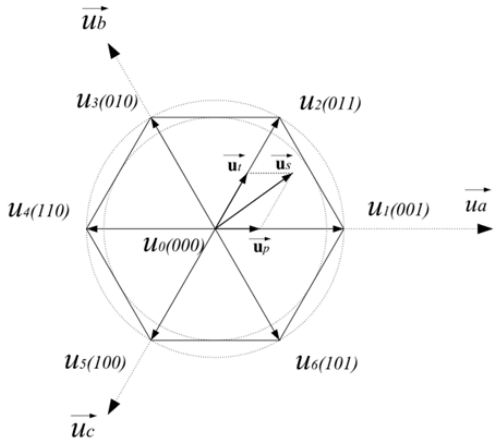

Fig. 3: Vectors control

Therefore, the control signal u_s is constrained by the inscribed circle within the hexagon (Fig. 3) and satisfies the following condition:

$$\mathbf{A}_{con}\mathbf{u}_s < \mathbf{B}_{con} \quad (10)$$

where

$$\mathbf{A}_{con} = \begin{bmatrix} 1 & 1/2 & -1/2 & -1 & -1/2 & 1/2 \\ -1/2 & 1/2 & 1 & 1/2 & -1/2 & -1 \\ -1/2 & -1 & -1/2 & 1/2 & 1 & 1/2 \end{bmatrix}^T$$

and

$$\mathbf{B}_{con} = \begin{bmatrix} 1 & 1 & 1 & 1 & 1 & 1 \end{bmatrix}^T$$

where $\mathbf{A}_{con}$ and $\mathbf{B}_{con}$ define the inverter limits. Applying the Park transformation for equation (10), the control constraints are formulated as (11)

$$\mathbf{A}_{con}\mathbf{T}\mathbf{u}_{dq} < \mathbf{B}_{con} \quad (11)$$

$$\text{Where: } \mathbf{T} = \begin{bmatrix} \cos\theta & -\sin\theta \\ \cos\theta - 2\pi/3 & -\sin\theta - 2\pi/3 \\ \cos\theta + 2\pi/3 & -\sin\theta + 2\pi/3 \end{bmatrix}$$

Substituting (8) into (9), we obtain the condition for the control signal u_{dq} with the constraint (11),

$$\begin{cases} \min J = \bar{\mathbf{u}}_{dq}^T \ k \ \mathbf{H}^T\mathbf{Q}\mathbf{H}\bar{\mathbf{u}}_{dq} \ k \\ +2 \ \mathbf{\Phi}\mathbf{i}_{dq} \ k \ + \mathbf{h}\psi_f - \mathbf{i}_{dq}^{ref} \ ^T \ \mathbf{Q}\mathbf{H}\bar{\mathbf{u}}_{dq} \ k \ + C \\ \mathbf{A}_{con}\mathbf{T}\mathbf{u}_{dq} < \mathbf{B}_{con} \end{cases} \quad (12)$$

Expression is the condition for determining the control signal u_{dq} for the current control loop. By applying optimization algorithms to solve the system of equations as (12), the desired optimal control signal is obtained.

3. Simulation Results

To validate the proposed controller, a simulation model was built in MATLAB/Simulink using the motor parameters presented in Table. 1. The simulation results will be performed with two test scenarios: a test with the independent current controller and a test with a position, speed, and current controller.

Table. 1: Motor parameters

Motor parameters	*Symbol*	*Value*	*Unit*
d-axis stator inductance	L_{sd}	1.4	mH
q-axis stator inductance	L_{sq}	1.4	mH
Stator resistance	R_s	10.3	Ω
Rotor flux	ψ_p	0.035	Wb
Number of pole pairs	z_p	2	
Pole step	τ_p	0.02	m

Case 1: simulation with the independent current controller.

The simulation scenario was conducted with variations in both currents i_d and i_q. Variation of i_d at t = 0.025s the reference current i_d was changed $i_d^{ref} = 1A$, at t = 0.075s the reference current i_d was changed $i_d^{ref} = -1A$. Variation of i_q: at t = 0s the reference current i_q was changed $i_q^{ref} = -1A$, at t = 0.005s the reference current i_q was changed $i_d^{ref} = 1A$.

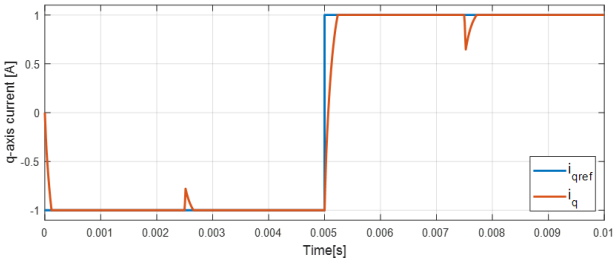

Fig. 4: Response of current i_q

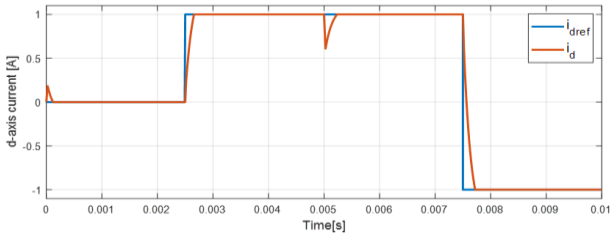

Fig. 5: Response of current i_d

The current response results for i_d and i_q in Fig. 4 and Fig. 5 shows the cross-coupling effects. However, these effects only occur during the transient phase. The current response was measured under two conditions: when i_d changes while i_q remains constant and when i_q changes while i_d remains constant. A response time of under 200µs was observed in both cases. These results validate the tracking performance of the proposed controller.

Case 2: Simulation with the all controller

A simulation scenario was designed to evaluate the system's response. This involved a straight-line trajectory with a constant speed of 200 mm/s to ensure trajectory differentiability. The motor first moved from 0 mm to 100 mm in 0.5 seconds, then held that position for 1 second. Finally, the motor returned to 0 mm in 0.5 seconds, again at 200 mm/s. A load force of 10 N was applied at t = 1s.

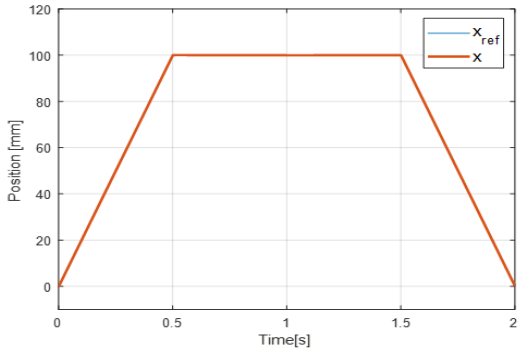

Fig. 6: The position response of the motor

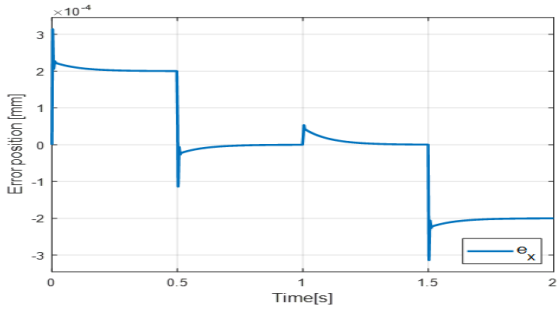

Fig. 7: The error position of the motor.

Fig. 6 shows the motor's trajectory and response, demonstrating its ability to track the reference trajectory. The maximum position error e_{xmax} = 0.3 mm meets the specified performance criteria (Fig. 7).

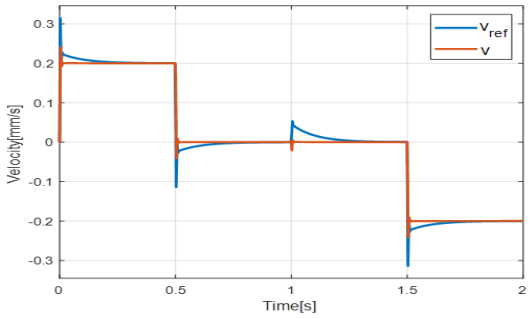

Fig. 8: The speed response of the motor.

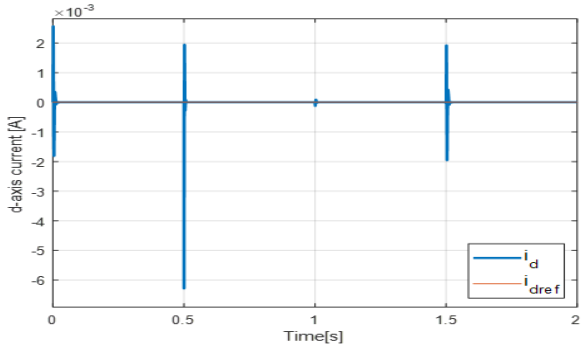

Fig. 9: Response of current i_d

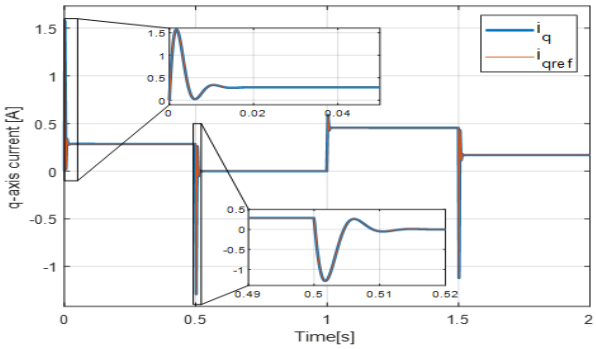

Fig. 10: Response of current i_q

The fast current convergence enables the outer loop controller to achieve the desired quality response rapidly (Fig 8). Fig. 9 and Fig. 10 show the current's response time to outer loop controller changes. The current loop's reaction is virtually instantaneous concerning changes directed by the speed loop.

4. Conclusion

In this paper, a control strategy for a tubular linear motor has been proposed and developed. The constraints imposed by the limitations of the power converter have been analyzed and mathematically formulated. Additionally, the discrete model of the motor has been presented. Based on this foundation, a Constrained Control Set Model Predictive Controller (CCS-MPC) has been applied. The proposed controller has demonstrated its effectiveness through simulation results, achieving a current response time of less than 200µs. These results are promising for future applications in experimental models.

Conflict of interest

The authors declared "No conflict of interest".

Acknowledgment

The authors gratefully acknowledge Thai Nguyen University of Technology, Vietnam, for supporting this work.

References

[1] H. Tobias, and J. Wallaschek "Survey of the present state of the art of piezoelectric linear motors", *Ultrasonics*, Vol. 38, No. 1-8, pp. 37-40, 2000. https://doi.org/10.1016/S0041-624X(99)00143-2

[2] P. K. Budig "The application of linear motors", *Proceedings IPEMC 2000. Third International Power Electronics and Motion Control Conference (IEEE Cat. No.00EX435)*, Beijing, China, pp. 1336-1341, 2000. https://doi.org/10.1109/IPEMC.2000.883044

[3] W. Xiuping, S. Yao, C. Qu, Y. Wang, Z. Xu, W. Huang and H. Wang "Direct thrust force control of primary permanent magnet linear motor based on improved extended state observer and model-free adaptive predictive control", *Actuators*, Vol. 11, No. 10, art. no. 270, 2022. https://doi.org/10.3390/act11100270

[4] J. Atencia, M. M. Iturralde, G. Martinez, A. Garcia Rico, and J. Florez "Control strategies for positioning of linear induction motor: tests and discussion", *IEEE International Electric Machines and Drives Conference*, Vol. 3, pp. 1651-1655, 2003. https://doi.org/10.1109/IEMDC.2003.1210673

[5] G. Kang and K. Nam "Field-oriented control scheme for linear induction motor with the end effect", *IEE Proceedings Electric Power Applications*, Vol. 152, No. 6, pp. 1565-1572, 2005. [CrossRef] https://doi.org/10.1049/ip-epa:20045185

[6] Y. W. Zhu and Y. H. Cho "Thrust Ripples Suppression of Permanent Magnet Linear Synchronous Motor", *IEEE Transactions on Magnetics*, Vol. 43, No. 6, pp. 2537-2539, 2007. https://doi.org/10.1109/TMAG.2007.893308

[7] J. J. Gorman, and N. G. Dagalakis "Force control of linear motor stages for microassembly", *ASME international mechanical engineering congress and exposition*, Vol. 37130, pp. 615-623, 2003. https://doi.org/10.1115/IMECE2003-42079

[8] W. Wang, Y. Feng, Y. Shi, M. Cheng, W. Hua and Z. Wang "Direct Thrust Force Control of Primary Permanent-Magnet Linear Motors With Single DC-Link Current Sensor for Subway Applications", *IEEE Transactions on Power Electronics*, Vol. 35, No. 2, pp. 1365-1376, 2020. https://doi.org/10.1109/TPEL.2019.2923378

[9] L. Cui, H. Zhang and D. Jiang "Research on High Efficiency V/f Control of Segment Winding Permanent Magnet Linear Synchronous Motor", *IEEE Access*, Vol. 7, pp. 138904-138914, 2019. https://doi.org/10.1109/ACCESS.2019.2930047

[10] R. C. Creppe, J. A. C. Ulson and J. F. Rodrigues, "Influence of Design Parameters on Linear

Induction Motor End Effect", *IEEE Transactions on Energy Conversion*, Vol. 23, No. 2, pp. 358-362, 2008. https://doi.org/10.1109/TEC.2008.918594

[11] A. H. Selcuk and H. Kurum "Investigation of End Effects in Linear Induction Motors by Using the Finite-Element Method", *IEEE Transactions on Magnetics*, Vol. 44, No. 7, pp. 1791-1795, 2008. https://doi.org/10.1109/TMAG.2008.918277

[12] L. Zeng, X. Chen, X. Li, W. Jiang and X. Luo "A Thrust Force Analysis Method for Permanent Magnet Linear Motor Using Schwarz–Christoffel Mapping and Considering Slotting Effect, End Effect, and Magnet Shape", *IEEE Transactions on Magnetics*, Vol. 51, No. 9, pp. 1-9, 2015. https://doi.org/10.1109/TMAG.2015.2432151

[13] H. Dong, X. Yang and M. V. Basin "Practical Tracking of Permanent Magnet Linear Motor Via Logarithmic Sliding Mode Control", *IEEE/ASME Transactions on Mechatronics*, Vol. 27, No. 5, pp. 4112-4121, 2022. https://doi.org/10.1109/TMECH.2022.3142175

[14] K. Shao, J. Zheng, H. Wang, F. Xu, X. Wang, and B. Liang "Recursive sliding mode control with adaptive disturbance observer for a linear motor positioner", *Mechanical Systems and Signal Processing*, Vol. 146, art. no. 107014, 2021. https://doi.org/10.1016/j.ymssp.2020.107014

[15] K. Shao, J. Zheng, H. Wang, X. Wang, R. Lu and Z. Man "Tracking Control of a Linear Motor Positioner Based on Barrier Function Adaptive Sliding Mode", *IEEE Transactions on Industrial Informatics*, Vol. 17, No. 11, pp. 7479-7488, 2021. https://doi.org/10.1109/TII.2021.3057832

[16] L. Yu, J. Huang, W. Luo, S. Chang, H. Sun, and H. Tian "Sliding-mode control for PMLSM position control - A review", *Actuators*, Vol. 12, No. 1, art. no. 31, 2023. https://doi.org/10.3390/act12010031

[17] A. Accetta, M. Cirrincione, F. D'Ippolito, M. Pucci and A. Sferlazza "Input–Output Feedback Linearization Control of a Linear Induction Motor Taking Into Consideration Its Dynamic End-Effects and Iron Losses", *IEEE Transactions on Industry Applications*, Vol. 58, No. 3, pp. 3664-3673, 2022. https://doi.org/10.1109/TIA.2022.3160409

[18] H. Gao, Y. Liu, W. Sun and X. Yu "Adaptive Wavelet Tracking Control of Dual-Linear-Motor-Driven Gantry Stage With Suppression of Crossbeam Rotation", *IEEE/ASME Transactions on Mechatronics*, Vol. 29, No. 1, pp. 97-105, 2024. https://doi.org/10.1109/TMECH.2023.3293568

[19] Z. Liu, W. Lin, X. Yu, J. J. Rodríguez-Andina and H. Gao "Approximation-Free Robust Synchronization Control for Dual Linear Motors Driven Systems With Uncertainties and Disturbances", *IEEE Transactions on Industrial Electronics*, Vol. 69, No. 10, pp. 10500-10509, 2022. https://doi.org/10.1109/TIE.2021.3137619

[20] M. A. M. Cheema, and J. E. Fletcher "Advanced direct thrust force control of linear permanent magnet synchronous motor", *Springer International Publishing*, 2020. https://doi.org/10.1007/978-3-030-40325-6

***